Environmental Science & Technology

Article

pubs.acs.org/est

Effect of Gravity on Colloid Transport through Water-Saturated Columns Packed with Glass Beads: Modeling and Experiments

Constantinos V. Chrysikopoulos*,† and Vasiliki I. Syngouna‡

†School of Environmental Engineering, Technical University of Crete, 73100 Chania, Greece

‡Environmental Engineering Laboratory, Department of Civil Engineering, University of Patras, 26500 Patras, Greece

Supporting Information

ABSTRACT: The role of gravitational force on colloid transport in water-saturated columns packed with glass beads was investigated. Transport experiments were performed with colloids (clays: kaolinite KGa-1b, montmorillonite STx-1b). The packed columns were placed in various orientations (horizontal, vertical, and diagonal) and a steady flow rate of Q = 1.5 mL/min was applied in both up-flow and down-flow modes. All experiments were conducted under electrostatically unfavorable conditions. The experimental data were fitted with a newly developed, analytical, one-dimensional, colloid transport model. The effect of gravity is incorporated in the mathematical model by combining the interstitial velocity (advection) with the settling velocity (gravity effect). The results revealed that flow direction influences colloid transport in porous media. The rate of particle deposition was shown to be greater for up-flow than for down-flow direction, suggesting that gravity was a significant driving force for colloid deposition.

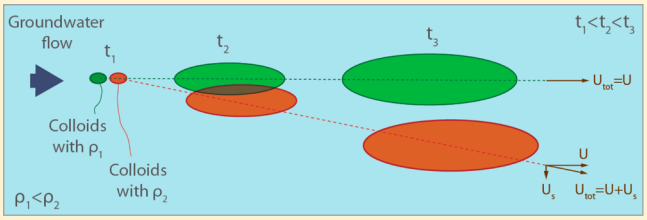

INTRODUCTION

The transport of colloids in porous and fractured media has long been recognized to be of considerable importance to a number of environmental practical applications, including groundwater pollution by microbial pathogens, in situ bioremediation of contaminated aquifers, and granular filtration of water and wastewater. The factors that influence colloid transport in saturated as well as unsaturated porous, and fractured media are quite complex. Numerous investigators have examined theoretically and experimentally the various factors that affect colloid transport in porous and fractured media, especially the effects of interstitial velocity,[1−4] colloid particle size,[5−9] collector size,[4,10−12] solid matrix porosity,[13] collector roughness,[9,14−16] ionic strength,[2,17−20] water chemistry,[21−23] gravitational settling,[24−28] and presence of suspended clays.[3,29−32]

The effect of flow direction on colloid fate and transport in porous media has received relatively minor attention. However, laboratory experiments with bench-scale model aquifers are traditionally conducted with flow direction orthogonal to gravity (horizontal flow),[33−35] whereas packed column experiments are carried out with flow orthogonal to gravity,[4,30,31,36] against gravity (up-flow),[7,23,37−42] or in the direction of gravity (down-flow).[43−47] The up-flow direction is widely used because packed columns are traditionally saturated using up-flow to reduce air entrapment. However, numerous of the published studies do not report the flow direction used, and either neglect or regard insignificant the influence of gravitational settling, which is potentially a significant retention mechanism. Experimental data published in the literature are frequently compared to the colloid filtration theory (CFT) without careful consideration of the experimental flow direction. It should be noted that CFT was developed for conditions where the flow is in the direction of gravity.

Very few studies have examined the effect of gravity on colloid sedimentation and transport in fractured and porous media. Wan et al.[24] developed a model to predict colloid sedimentation in porous media and suggested that the sedimentation mechanism can be quite significant for bacteria transport, especially, in studies of long-term downward bacterial transport, and can explain the presence of bacterial populations, which have been observed in deep subsurface environments. Chen et al.[25] examined the role of gravity on the deposition of colloids and bacteria onto glass surfaces of a rectangular parallel plate flow chamber system under electrostatically favorable and unfavorable conditions and concluded that gravity was a significant driving force for particle deposition. James and Chrysikopoulos[26] used a particle tracking technique to simulate the colloid transport in a bifurcating fracture, and shown that dense colloids preferentially exit fractures that are gravitationally down gradient. James and Chrysikopoulos[27] conducted numerical experiments to examine the effects of gravity on dense polydisperse colloid transport in a fracture, and concluded that fracture angle (angle of flow orientation relative to gravity) can significantly impact colloid transport. Ma et al.[28] performed unit model simulations to examine the effect of gravity on colloid retention and concluded that the Happel

Received: March 16, 2014
Revised: May 23, 2014
Accepted: May 23, 2014
Published: May 23, 2014

sphere-in-cell model is more sensitive to flow orientation relative to gravity than the hemispheres-in-cell model. It should be noted that the Happel sphere-in-cell model assumes that a solid sphere is surrounded by a fluid-layer with thickness adjusted so that the unit cell porosity is equal to the porous medium porosity, and that the flow is in the direction of gravity,[48] whereas the hemispheres-in-cell model assumes that the unit cell consists of two solid hemispheres in contact surrounded by a fluid layer of adjustable thickness, and that the flow is in the direction of gravity, perpendicular to the line connecting the two hemisphere centers.[49]

Although there are numerous mathematical models available that describe colloid transport in porous media, in this study, the frequently employed continuum approach was adopted. The phenomenological colloid transport model developed by Sim and Chrysikopoulos[50] was extended to account for colloid sedimentation, in order to examine how the flow direction influences colloid fate and transport in porous media. To our knowledge, clay mineral transport in columns packed with glass beads under various flow directions, and electrostatically unfavorable conditions has not been previously explored.

MATHEMATICAL DEVELOPMENT

Transport of Dense Colloids. Based on the continuum approach, the transport of colloids (including biocolloids) in one-dimensional, homogeneous, water saturated porous media with first-order attachment (or filtration) and inactivation, assuming that an effective velocity term accounts for both the interstitial as well as the particle settling velosity is governed by the following partial differential equation:

$$\frac{\partial C(t,x)}{\partial t} + \frac{\rho_b}{\theta}\frac{\partial C^*(t,x)}{\partial t} = D\frac{\partial^2 C(t,x)}{\partial x^2} - U_{tot}\frac{\partial C(t,x)}{\partial x} - \lambda C(t,x) - \lambda^*\frac{\rho_b}{\theta}C^*(t,x) \quad (1)$$

where C [M/L^3] is the concentration of colloids in suspension; C^* [M/M] is the concentration of colloids attached on the solid matrix; t [t] is time; ρ_b [M/L^3] is the bulk density of the solid matrix; θ [−] is the porosity of the porous medium; D [L^2/t] is the hydrodynamic dispersion coefficient; λ [1/t] is the transformation rate constant of suspended colloids (e.g., inactivation, which refers to loss of infective capability or die-off of suspended biocolloids); λ^* [1/t] is the transformation rate constant of colloids attached on the solid matrix; and U_{tot} [L/t] is the total (or effective) particle velocity, which for colloids subject to gravitational forces accounts for gravitational settling:

$$U_{tot} = U + U_{s(\mathbf{i})} \quad (2)$$

where U [L/t] is the interstitial velocity, and $U_{s(\mathbf{i})}$ [L/t] is a modified version of the traditional "free particle" settling velocity in static water columns,[51] to "restricted particle" settling in granular porous media under directional flow conditions:

$$U_{s(\mathbf{i})} = -f_s\frac{(\rho_p - \rho_w)d_p^2}{18\mu_w}g_{(\mathbf{i})} \quad (3)$$

where f_s [-] is the correction factor accounting for particle settling in the presence of the solid matrix of granular porous media, ρ_w [M/L^3] and ρ_p [M/L^3] are the densities of the suspending fluid (water) and the colloid particle, respectively; μ_w [M/(L·t)] is the dynamic viscosity of water, and $g_{(\mathbf{i})}$ [L/t^2] is the gravity vector along the direction of the interstitial flow defined as

$$g_{(\mathbf{i})} = g_{(-z)}\sin\beta\mathbf{i} \quad (4)$$

where $g_{(-z)}$ [M/t^2] is the acceleration due to gravity in the negative z-direction (indicated by the subscript in parentheses), β [°] is the angle of the main flow direction with respect to the horizontal x-direction, and $\mathbf{i}$ is the unit vector parallel to the flow (see definition sketch Figure SI1 in the Supporting Information). For up-flow $0° < \beta < 90°$, whereas for down-flow $-90° < \beta < 0°$. Furthermore, it should be noted that for the case of diagonal (or inclined) orientation, although the gravity vector component $g_{(\mathbf{i})} = g_{(-z)}\sin\beta\mathbf{i}$, is accounted for in the one-dimensional model as gravity effect, the vector component $g_{(-\mathbf{j})} = -g_{(-z)}\cos\beta\mathbf{j}$, is not necessarily balanced and can cause colloid deposition or lateral dispersion. The vector component $g_{(-\mathbf{j})}$ cannot be considered in the one-dimensional model used in this study.

The correction factor f_s [−] converts the average free particle sedimentation velocity to the average sedimentation velocity through water saturated porous media:[24]

$$f_s = \frac{b + 0.67}{b + 0.93/\varepsilon} \quad (5)$$

where b represents the ratio of the average free settling segment length to the grain radius, and ε [−] ($0 \le \varepsilon \le 1$) is an empirical correction factor arising from influences of the grain surface. It should be noted that $f_s \approx 0.9$ when the grains of the granular porous media contribute only to tortuosity and do not provide additional frictional resistance.[24]

It should be noted that the governing colloid transport eq 1 is essentially the colloid transport model provided by Sim and Chrysikopoulos[50] with U replaced by U_{tot}. Also, eq 3 is the balance among gravity, buoyancy and viscous forces, implicitly assumes that the colloids are small, uniform spheres, and there is a distinct density difference between the colloids and the suspending fluid. The rate of colloid attachment onto the solid matrix is described by the following first-order equation:[52,53]

$$\frac{\rho_b}{\theta}\frac{\partial C^*(t,x)}{\partial t} = k_c C(t,x) - k_r\frac{\rho_b}{\theta}C^*(t,x) - \lambda^*\frac{\rho_b}{\theta}C^*(t,x) \quad (6)$$

where k_c [1/t] is the attachment rate constant, and k_r [1/t] is the detachment rate constant.

The initial and boundary conditions employed are

$$C(0,x) = 0 \quad (7)$$

$$-D\frac{\partial C(t,0)}{\partial x} + U_{tot}C(t,0) = \begin{cases} U_{tot}C_0 & 0 < t \le t_p \\ 0 & t > t_p \end{cases} \quad (8)$$

$$\frac{\partial C(t,\infty)}{\partial x} = 0 \quad (9)$$

where C_0 [M/L^3] is the source concentration of colloids suspended in the aqueous phase, and t_p [t] is the colloid broad pulse duration. The first condition (7) states that porous medium is initially free of colloids. Condition (8) is a typical

constant flux boundary condition, which implies concentration discontinuity at the inlet of the porous medium.[54] Condition (9) describes that a concentration-continuity is preserved at the downstream boundary of the semi-infinite porous medium. The analytical solution to the partial differential eqs 1 and 6, subject to the initial and boundary conditions (7)−(9), with U instead of U_{tot}, has been derived by Sim and Chrysikopoulos,[50] which is given by equation (SI1) in the Supporting Information.

It should be noted that the present colloid transport model is different from traditional models only in the velocity term, U_{tot}, which is essentially an effective velocity and accounts for both the interstitial velocity as well as the free particle settling velocity. The various model parameters can be estimated by fitting the analytical solution to the experimental data with the nonlinear least-squares regression package "ColloidFit",[50] which can be obtained for free from the authors upon request.

Moment Analysis. The tracer and colloid concentrations collected at the column exit were analyzed by the absolute temporal moments:

$$m_n(L) = \int_0^\infty t^n C(L, t)\mathrm{d}t \tag{10}$$

where the subscript n = 0, 1, 2, ... indicates the order of the moment, and L [L] is the porous medium (column) length. Note that the zeroth absolute temporal moment, m_0 [tM/L^3], describes the mass of colloids in the breakthrough curve. The first absolute moment, m_1 [t^2 M/L^3], is the mean residence time. The second absolute temporal moment, m_2 [t^3 M/L^3], describes the spreading of colloids in the breakthrough curve. The normalized temporal moments are given by the following expression:[27]

$$M_n(L) = \frac{m_n(L)}{m_0(L)} = \frac{\int_0^\infty t^n C(L, t)\mathrm{d}t}{\int_0^\infty C(L, t)\mathrm{d}t} \tag{11}$$

The first normalized temporal moment, M_1 [t], characterizes the center of mass of the concentration distribution curve and defines the average velocity. The second normalized temporal moment, M_2 [t^2], characterizes the spreading of the concentration distribution curve. Worthy to note is that the ratio $M_{1(c)}/M_{1(t)}$ indicates the degree of velocity enhancement of colloid relative to the conservative tracer, where the subscript (c) indicates colloid, and (t) tracer. If this ratio is less than one, there exists colloid retardation, and if it is greater than one there exists velocity enhancement of colloid transport. Furthermore, the mass recovery, M_r [−], of the tracer or the suspended particles is quantified by the following expression:

$$M_r(L) = \frac{m_0(L)}{C_0 t_p} \tag{12}$$

Model Simulations. To illustrate the effect of gravity on restricted particle settling in porous media, eq 3 was plotted in Figure 1 as a function of the angle of the main flow direction for both down-flow and up-flow directional flow conditions for hypothetical, relatively dense colloid particles, bacteria and viruses. It should be clarified here that the restricted particle settling is affected by particle size but also by particle density. Therefore, as shown in Figure 1, the restricted particle settling of colloids and bacteria is affected by gravity, but the settling of small virus particles is practically unaffected by gravity. As expected, $U_{s(i)}$ is positive for down-flow conditions and negative for up-flow conditions; whereas, for horizontal flow $U_{s(i)}$ = 0.

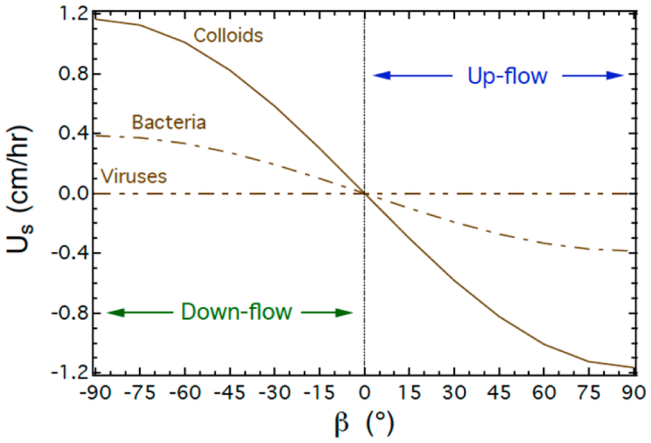

Figure 1. Restricted particle settling velocity as a function of column orientation and flow direction for colloids (clay: d_p = 2 μm, ρ_p = 2.65 g/cm^3), bacteria (*P. putida*: d_p = 2.2 μm, ρ_p = 1.45 g/cm^3), and viruses (bacteriophage MS2: d_p = 25 nm, ρ_p = 1.42 g/cm^3). Here f_s = 0.9.

Consequently, U_{tot} > U for down-flow conditions, U_{tot} < U for up-flow conditions, and U_{tot} = U for horizontal flow.

The analytical solution (SI1), presented in the Supporting Information, is used to illustrate the effect of gravity and flow direction on the transport of dense colloid particles in porous media. The model simulations presented in Figure 2 indicate

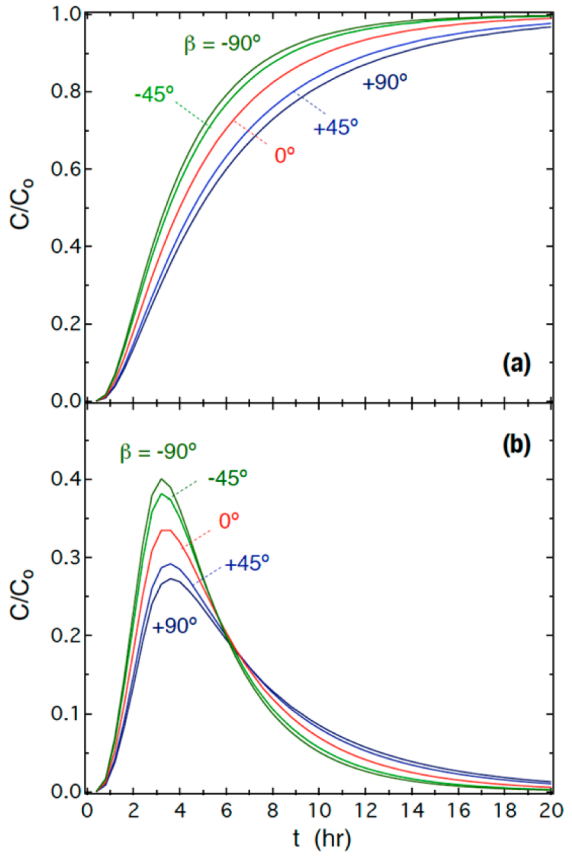

Figure 2. Simulations of normalized colloid break through curves for packed columns with various orientations and flow directions under: (a) continuous, and (b) broad pulse inlet boundary conditions. Here U = 4 cm/h, D = 22.5 cm^2/h, θ = 0.45, ρ_b = 1.63 g/cm^3, $\lambda = \lambda^*$ = 0 h^{-1}, $k_c = k_r$ = 0 h^{-1}, x = 15 cm, d_p = 5 μm, ρ_p = 1.15 g/cm^3, and t_p = 2 h.

dx.doi.org/10.1021/es501295n | Environ. Sci. Technol. 2014, 48, 6805−6813

Table 1. Physical Characteristics and Properties of Glass Beads, KGa-1b and STx-1b

parameter	values	reference
hydrodynamic diameter, d_p	KGa-1b: 843 ± 126 nm	59
	STx-1b: 1187 ± 381 nm	59
diameter, d_c	glass beads: 2 mm	31
zeta potential at pH 7, ζ	KGa-1b: −26.03 ± 2.77 mV	59
	STx-1b: −20.5 ± 0.8 mV	59
	glass beads:-54.6 ± 2.4 mV	31
isoelectric point, IEP	KGa-1b: pH 2.1	59
	STx-1b: nm[a]	59
particle density, ρ_p	2.2 g/cm^3	56
BET specific surface area	KGa-1b: 10.1 m^2/g	56
	STx-1b: 82.9 m^2/g	57
cation exchange capacity	KGa-1b: 2 mequiv/100 g	56
	STx-1b: 84.4 mequiv/100 g	56
morphology/Shape of <2 μm clay fraction	KGa-1b: hexagonal platy particles	59
	STx-1b: irregular thin flaky particles	59
chemical composition	KGa-1b: SiO_2 45.41%, Al_2O_3 38.79%, TiO_2 0.28%, Fe_2O_3 0.21%, MgO 0.01%, Na_2O 0.21%, K_2O 0.2%.	59
	STx-1b: SiO_2 72.92%, Al_2O_3 15.34%, TiO_2 0.13%, Fe_2O_3 0.75%, MnO 0.17%, MgO 3.69%, CaO 1.61%, Na_2O 0.29%, K_2O 0.1%, P_2O_5 0.05%, S 0.05%.	59
contact angle, β	$\beta_{KGa\text{-}1b}$: 46.1°	60
	$\beta_{STx\text{-}1b}$: 20.5 ± 2.8°	60
	$\beta_{glass\ beads}$: 32 ± 5°	61

[a]nm: Not measured.

that flow direction can significantly affect the transport of dense and/or large colloids. Clearly, there is faster breakthrough for down-flow (see Figure 2a), and lower peak colloid concentrations at the column exit for up-flow (see Figure 2b).

EXPERIMENTAL APPROACH

Clay Colloid Selection and Preparation. The clays used in this study were kaolinite (KGa-1b, is a well-crystallized kaolin from Washington County, Georgia),[55] and montmorillonite (STx-1b, a Ca-rich montmorillonite, white, from Gonzales County, Texas), purchased from the Clay Minerals Society, Columbia, MO. KGa-1b has a specific surface area of 10.1 m^2/g, and a cation exchange capacity of 2.0 mequiv/100 g.[56] STx-1b has a specific surface area of 82.9 m^2/g,[57] and assuming that the characteristics of STx-1b are comparable to those of STx-1, which is the previous batch of montmorillonite from the same area, its cation exchange capacity is 84.4 mequiv/100 g.[56]

Fifty grams of each clay mineral were mixed with 100 mL distilled deionized water (ddH_2O) in a 2 L beaker. Sufficient hydrogen peroxide (30%, solution) was added to oxidize all organic matter. The mineral suspension was adjusted to pH 10 with 0.1 M NaOH solution and dispersed by ultrasonication for 20 min. Subsequently, the suspension was diluted to 2 L and after 1 h sedimentation of the large clay particles, the supernatant containing the <2 μm colloidal fraction was flocculated by adding 0.5 M $CaCl_2$ solution. The colloidal particles were collected and washed with ddH_2O and ethanol to remove the Cl^- ions and subsequently dried at 60 °C.[58] The hydrodynamic diameters of the clay particles, were determined by the zetasizer to be d_p = 843 ± 126 nm for KGa-1b, and d_p = 1187 ± 381 nm for STx-1b.[31] The optical density of the clay colloids was analyzed at a wavelength of 280 nm by a UV-vis spectrophotometer, and the corresponding clay concentrations were determined twice as outlined by Chrysikopoulos and Syngouna.[59] The colloid suspensions were prepared in high-purity distilled deionized Milli-Q water (ddH_2O) with specific conductivity of 0.055 μS/cm, ensuring that the pH is close to neutral, which actually ranged between 6.7 and 7. The electrokinetic features (zeta potentials) of the clay colloid suspensions in ddH_2O are unfavorable to deposition (negative zeta potentials, high DLVO energy barriers) at pH > 2.1.[59] Therefore, a potential increase in the effluent pH from 7 to ∼9, due to possible mineral release from the glass beads during the column experiments, is not expected to alter the desired (unfavorable to deposition) conditions of this study. It should be noted that the zeta potential of the two clay colloids does not change significantly over the pH range 7−9.[59]

The zeta potential of the clays were measured in triplicates at the experimental conditions (pH 7, I_s = 0.1 mM) by a zetasizer (Nano ZS90, Malvern Instruments): −26.03 ± 2.77 mV for KGa-1b, and −20.5 ± 0.8 mV for STx-1b. The zeta potential of glass beads stored in ddH_2O at pH 7 is −54.6 ± 2.4 mV.[31] The isoelectric point (IEP) of KGa-1b in ddH_2O is pH_{IEP} = 2.1.[59] Following the work by Syngouna and Chrysikopoulos,[31] it was determined, based on the conventional DLVO and XDLVO interaction models, using electrokinetic zeta potentials instead of the surface potentials, that for pH 7 and I_s = 0.1 mM, repulsive electrostatic forces exist between the two clay colloids (KGa-1b, STx-1b) and the glass beads. A complete list of the physical characteristics and properties of the glass beads, KGa-1b and STx-1b is presented in Table 1.

Column Experiments. Flow through experiments were carried out with KGa-1b and STx-1b clays as model colloids in a 2.5 cm diameter and 30 cm long Chromaflex glass column packed with 2 mm in diameter glass beads (Fisher Scientific, New Jersey). Glass beads were chosen as model porous media because they are chemically nonreactive with the solutions used in this study. Prior to the experiments, the beads were cleaned with 0.1 M HCl for 3 h to remove surface impurities (e.g., iron hydroxide and organic coatings) that could promote physicochemical deposition of colloids, rinsed with ddH_2O, then soaked in 0.1 M NaOH for 3 h and rinsed with ddH_2O again. After the cleaning steps, the beads were dried in an oven

dx.doi.org/10.1021/es501295n | Environ. Sci. Technol. 2014, 48, 6805−6813

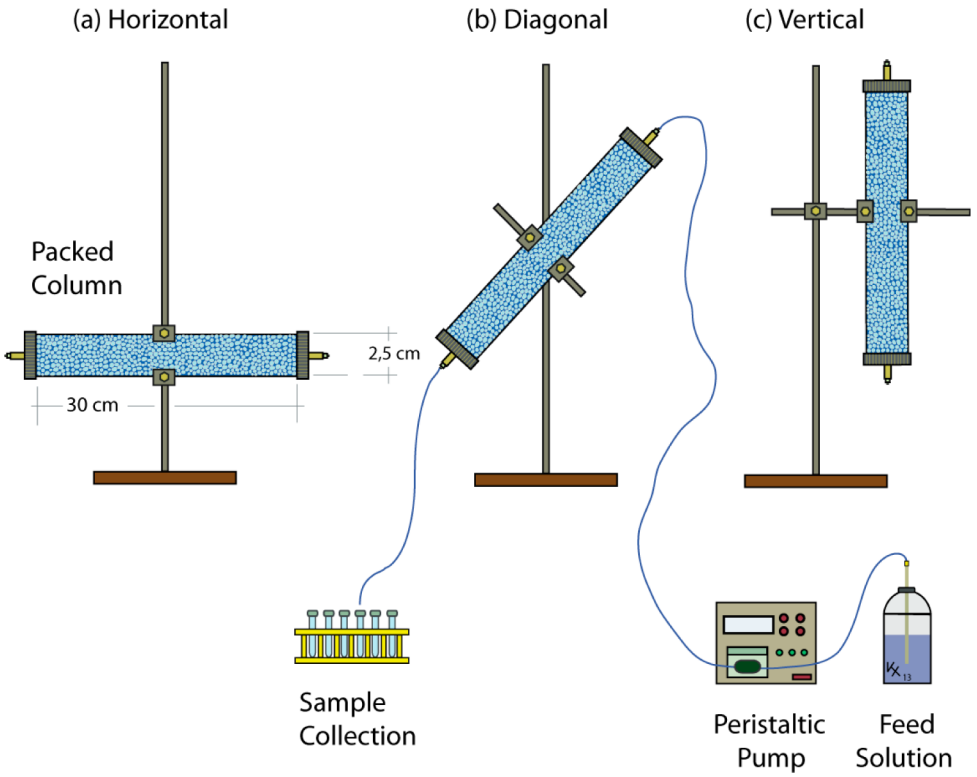

Figure 3. Experimental setup showing the various column arrangements: (a) horizontal, (b) diagonal, and (c) vertical.

at 105 °C and then stored in screw cap sterile beakers until use in the column experiments.

Each column was packed with glass beads under standing ddH_2O to minimize air entrapment. The estimated dry bulk density was 1.61 g/cm^3, and the estimated porosity of the various packed columns used in this study was in the range 0.41−0.42. Also, three pore volumes of sterile ddH_2O (pH 7, I_s = 0.1 mM) were passed through the column prior to each flow through experiment. The entire packed column as well as all the glassware and materials used for the experiments were sterilized in an autoclave at 121 °C for 20 min. Constant flow of sterile ddH_2O at flow rate of Q = 1.5 mL/min, corresponding to pore water velocity of U = 0.74 cm/min, was maintained through the packed column with a peristaltic pump. For each experiment, three pore volumes of the clay colloid suspension were injected into the packed column, followed by three pore volumes of ddH_2O. Note that the columns were placed horizontally (β = 0°), vertically (β= ± 90°), and inclined (β= ± 45°), as shown in Figure 3. A fresh column was packed for each experiment.

Chloride, in the form of potassium chloride, was chosen as the nonreactive tracer for the transport column experiments. The nonreactive tracer solution was prepared with 0.01 M KCl in ddH_2O. Chloride concentrations were measured using ion chromatography (ICS-1500, Dionex Corp., Sunnyvale, CA). One set of flow through experiments was performed with clay colloid transport in horizontal (β = 0°), a second set in vertical (β = ± 90°), and a third set in inclined (β= ± 45°) columns. For all sets, three pore-volumes of solution were injected into the packed column, followed by three pore volumes of ddH_2O. All experiments were carried out at room temperature (~25 °C).

EXPERIMENTAL RESULTS AND DISCUSSION

The normalized KGa-1b and STx-1b flowthrough experimental data are presented in Figure 4, together with the fitted model predictions. The parameters U_{tot}, D and k_c were estimated with the nonlinear least-squares regression package "ColloidFit" by fitting the analytical solution Supporting Information eq SI1 to the experimental KGa-1b and STx-1b breakthrough concentrations. Note that in order to keep the number of the fitted parameters equal to three (fitting more than three parameters does not lead to reliable and unique estimates), it was assumed that k_r, λ, and λ* are negligible.[4] The fitted parameters U_{tot}, D, and k_c together with their corresponding 95% confidence intervals are listed in Table 2. Traditionally, packed column dispersion coefficients are determined from tracer behavior; however, in this study, although tracer experiments were conducted and analyzed, the dispersion coefficient for the colloid transport data collected was treated as a fitted parameter, because colloid dispersivities are significantly different than tracer dispersivities.[7] From the fitted U_{tot} values listed in Table 2, the fitted restricted particle setling velocity was easily obtained as $U_{s(i)} = U_{tot} - 0.74$ cm/min, because for all experiments of this study U was fixed at 0.74 cm/min. Note that $U_{s(i)}$ is a function of both colloid size and density.

From Table 2 it is evident that all fitted U_s values followed the theoretical trend suggested by eq 3 ($U_{s(i)} = 0$ for horizontal flow, $U_{s(i)} > 0$ for down-flow, and $U_{s(i)} < 0$ for up-flow). A comparison between the fitted and theoretically determined $U_{s(i)}$ values is graphically illustrated in Figure 5. Based on the fitted k_c values listed in Table 2, particle attachment is generally higher for up-flow than down-flow experiments. This observation is in agreement with the results reported by Basha and Culligan[62] who conducted experiments under unfavorable conditions using smooth as well as rough bead packs, and observed that for down-flow experiments, straining

dx.doi.org/10.1021/es501295n | Environ. Sci. Technol. 2014, 48, 6805−6813

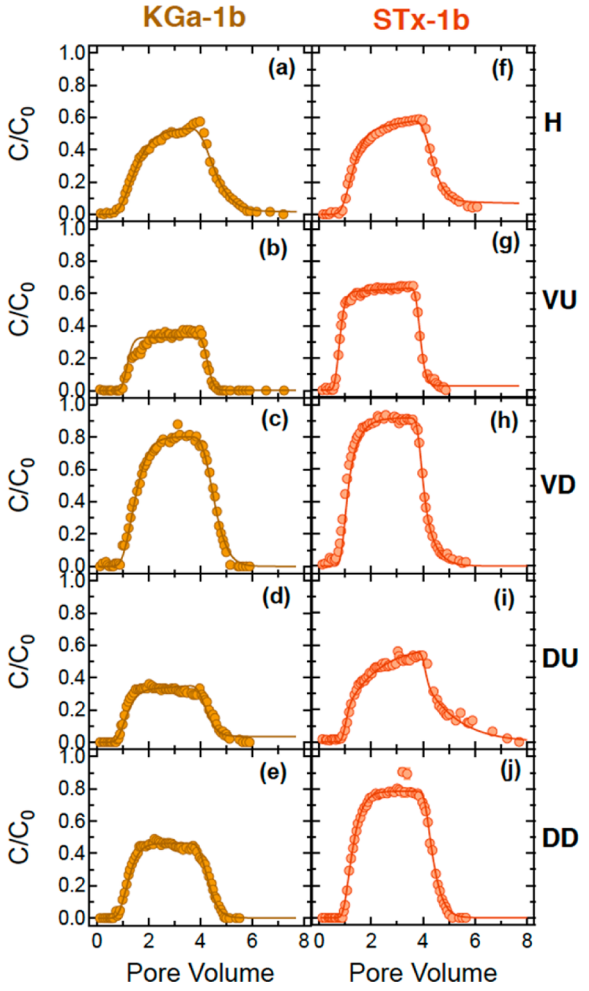

Figure 4. Experimental data (symbols) and fitted model simulations (curves) of (a–e) KGa-1b and (f–j) STx-1b breakthrough in columns packed with glass beads with (a,f) horizontal, (b,g) vertical up-flow, (c,h) vertical down-flow, (d,i) diagonal up-flow, and (e,j) diagonal down-flow directional flow conditions. Here, H-horizontal, VU-vertical up-flow, VD-vertical down-flow, DU-diagonal up-flow, DD-diagonal down-flow. Error bars are not shown because they are smaller than the size of the symbol.

was the primary filtration mechanism in the smooth bead packs, whereas, both straining and attachment by surface asperities were important filtration mechanisms in the rough bead packs, but roughness did not affect significantly the filtration process for up-flow experiments. In contrast, Ma et al.[28] found that colloidal deposition rate constants, under conditions favorable to deposition, were slightly higher for down-flow than up-flow experiments.

Only a fraction of the injected clay colloids was recovered at the column effluent, due to clay colloid deposition onto the glass beads. The calculated mass recovery, M_r, values listed in Table 2 suggested that there was more mass retained in the columns under upward than downward flows. With the exception of KGa-1b with VU mode (see exp. no 2 in Table 2), higher mass recoveries were observed for both clays for VD than DD flow directions, and for downward than upward flows. For the same flow conditions, higher retention of KGa-1b than STx-1b was observed (see Table 2), which could be attributed to the higher hydrophobicity of KGa-1b. This observation is in agreement with previous studies.[31,59] Furthermore, Syngouna and Chrysikopoulos[31] reported that the estimated Lewis acid–base free energy of interaction, $\Phi_{AB(h=h_0)}$, values are more negative for KGa-1b and glass beads (-42.2 mJ/m^2) than STx-1b and glass beads (-1.21 mJ/m^2). Therefore, KGa-1b–glass bead interaction is more hydrophobic than STx-1b-glass bead, because the polar Lewis acid–base free energy of interaction is a measure of the hydrophobic attraction between two surfaces.[63,64] However, it is worthy to note that, despite the highly unfavorable electrostatic conditions of the experiments conducted in this study, significant amount of both clays were retained in the packed columns, suggesting that physical retention was an important filtration mechanism. Clay retention was probably caused by straining and wedging, which are important mechanisms of mass loss in the packed columns when colloid to collector diameter ratios (d_p/d_c) are greater than 0.004,[65] or 0.003.[12] In this study, $d_p/d_c \leq 0.001$, which is comparable to the suggested threshold. Another possible explanation for the observed colloid retention is the planar shape of the clay particles, because colloid shape can influence colloid retention. For example, Seymour et al.[66] reported that collector surface roughness is responsible for the higher retention of non spherical than spherical colloid particles. Note that, both collector surface roughness, and surface charge heterogeneity are known to increase colloid filtration.[14,67−70]

The first normalized temporal moment for each breakthrough curve was calculated with eq 11. Also, the ratio of $M_{1(c)}$ for the two clays (KGa-1b, STx-1b) to $M_{1(t)}$ for the tracer Cl^- was computed for each flow direction employed (see Table 2). It is worthy to note that, with the exception of exp. no 7, velocity enhancement ($M_{1(c)}/M_{1(t)} > 1$) was observed for both of the clay colloids and all of the flow conditions considered in this study. The observed early breakthrough of the two clays, compared to the conservative tracer, is attributed to size exclusion.[7,37,71] The relatively large clay particles were excluded from small pores spaces, and sampled the more conductive ranges of the interstitial velocity distribution.[5] Consequently, the clay particles were transported faster than the conservative tracer.

Environmental Implications. A mathematical model describing colloid transport in water saturated porous media, accounting for the gravitational force was presented. The colloid transport model successfully matched the clay particles breakthrough data. The experimental results verified the theoretical prediction that gravity is a significant force for colloid transport in water saturated porous media under conditions unfavorable to deposition, especially for the larger and denser particles. It was shown that particle attachment is generally higher for up-flow than down-flow experiments, and that more mass is retained in porous media under upward than downward flows. Finally, it was shown that colloid particle velocities were enhanced compared to the tracer for most of the cases considered in this study. Although the fitted dispersion coefficients were larger for the clay particles considered in this study than the conservative tracer, chloride, more work is needed to fully describe the relationship between dispersivity and colloid particle size. Future studies should consider the role of gravitational force on colloid transport in saturated as well as unsaturated packed columns under different velocities and ionic strengths (electrostatically favorable conditions).

Table 2. Experimental Conditions, Fitted Parameter Values, and Estimated Mass Recoveries

exp. no	C_o mg/L (clays) mol/L (tracer)	flow direction[a]	U_{tot}[b] (cm/min)	$U_{s(i)}$[c] (cm/min)	D[b] (cm^2/min)	k_c[b] (1/min)	M_r[d] (%)	$M_{1(c)}/M_{1(t)}$[e]
			KGa-1b					
1	62.8	H	0.73741 ± 0.0018	0.00000	1.0614 ± 0.098	0.0103 ± 0.001	53.5	1.19
2	50.3	VU	0.73841 ± 0.0008	−0.00159	0.2968 ± 0.036	0.0236 ± 0.001	32.6	1.05
3	67.6	VD	0.74193 ± 0.0009	0.00193	0.5984 ± 0.026	0.0037 ± 0.001	79.5	1.12
4	56.6	DU	0.73474 ± 0.0015	−0.00526	0.6790 ± 0.063	0.0233 ± 0.001	37.6	1.07
5	66	DD	0.74330 ± 0.0016	0.00330	0.6554 ± 0.052	0.0153 ± 0.004	47.9	1.05
			STx-1b					
6	100.1	H	0.73895 ± 0.0004	0.00000	0.7377 ± 0.052	0.0123 ± 0.001	58.6	1.16
7	105.9	VU	0.73827 ± 0.0016	−0.00174	0.5521 ± 0.018	0.0164 ± 0.001	65	0.89
8	102.3	VD	0.74219 ± 0.0013	0.00219	0.5272 ± 0.029	0.0033 ± 0.001	93.8	1.01
9	75.9	DU	0.73264 ± 0.0023	−0.00736	1.1751 ± 0.094	0.0123 ± 0.001	61.5	1.31
10	82.5	DD	0.74439 ± 0.0026	0.00438	0.5157 ± 0.072	0.0048 ± 0.000	83.1	1.06
			Tracer					
	0.01	H	0.74016 ± 0.0001		0.1369 ± 0.033		100	
	0.01	VU, VD	0.73985 ± 0.0002		0.1671 ± 0.041		100	
	0.01	DU, DD	0.73995 ± 0.0001		0.1568 ± 0.031		100	

[a]H-horizontal, VU-vertical up-flow, VD-vertical down-flow, DU-diagonal up-flow, DD-diagonal down-flow. [b]Fitted with ColloidFit. [c]Evaluated with eq 2. [d]Evaluated with eq 12. [e]Evaluated with eq 11.

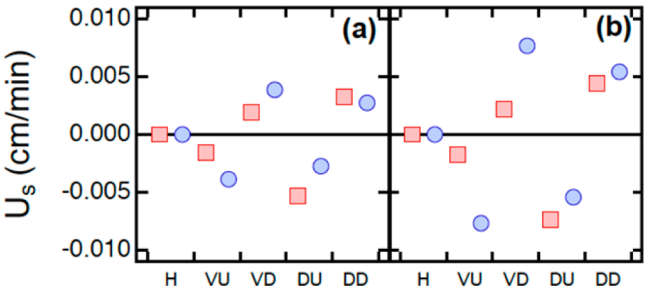

Figure 5. Comparison between theoretically estimated (circles), and fitted (squares) U_s values for: (a) KGa-1b, and (b) STx-1b. Here, $\rho_{KGa\text{-}1b} = \rho_{STx\text{-}1b} = 2.2$ g/cm^3. Here $U_{s(i)} < 0$ for up-flow and $U_{s(i)} > 0$ for down-flow experiments, H-horizontal, VU-vertical up-flow, VD-vertical down-flow, DU-diagonal up-flow, DD-diagonal down-flow.

■ ASSOCIATED CONTENT

Supporting Information

Classification of modeling approaches, definition sketch, and analytical solution. This material is available free of charge via the Internet at http://pubs.acs.org.

■ AUTHOR INFORMATION

Corresponding Author

*Phone: + 30 2821037797; e-mail: cvc@enveng.tuc.gr.

Notes

The authors declare no competing financial interest.

■ ACKNOWLEDGMENTS

This research has been cofinanced by the European Union (European Social Fund-ESF) and Greek National Funds through the Operational program "Education and Lifelong Learning" under the action Aristeia I (Code No. 1185). This work is a collaboration between members of the BioMet Network.

■ REFERENCES

(1) Tong, M.; Johnson, W. P. Colloid population heterogeneity drives hyperexponential deviation from classic filtration theory. *Environ. Sci. Technol.* **2007**, *41*, 493−499.

(2) Hendry, M.; Lawrence, J.; Maloszewski, P. Effects of velocity on the transport of two bacteria through saturated sand. *Groundwater* **1999**, *37*, 103−112.

(3) Walshe, G. E.; Pang, L.; Flury, M.; Close, M. E.; Flintoft, M. Effects of pH, ionic strength, dissolved organic matter, and flow rate on the cotransport of MS2 bacteriophages with kaolinite in gravel aquifer media. *Water Res.* **2010**, *44*, 1255−1269.

(4) Syngouna, V. I.; Chrysikopoulos, C. V. Transport of biocolloids in water saturated columns packed with sand: Effect of grain size and pore water velocity. *J. Contam. Hydrol.* **2011**, *126*, 301−314, DOI: 10.1016/j.jconhyd.2011.09.007.

(5) James, S. C.; Chrysikopoulos, C. V. Analytical solutions for monodisperse and polydisperse colloid transport in uniform fractures. *Colloids Surf., A* **2003**, *226*, 101−118, DOI: 10.1016/S0927-7757(03)00316-9.

(6) Jin, Y.; Flury, M. Fate and transport of viruses in porous media. *Adv. Agron.* **2002**, *77*, 39−102.

(7) Keller, A. A.; Sirivithayapakorn, S. S.; Chrysikopoulos, C. V. Early breakthrough of colloids and bacteriophage MS2 in a water-saturated sand column. *Water Resour. Res.* **2004**, *40*, W08304 DOI: 10.1029/2003WR002676.

(8) James, S. C.; Bilezikjian, T. K.; Chrysikopoulos, C. V. Contaminant transport in a fracture with spatially variable aperture in the presence of monodisperse and polydisperse colloids. *Stoch. Environ. Res. Risk Assess.* **2005**, *19* (4), 266−279, DOI: 10.1007/s00477-004-0231-3.

(9) Tong, M.; Johnson, W. P. Excess colloid retention in porous media as a function of colloid size, fluid velocity, and grain angularity. *Environ. Sci. Technol.* **2006**, *40*, 7725−7731.

(10) Harter, T.; Wagner, S.; Atwill, E. R. Colloid transport and filtration of *Cryptosporidium parvum* in sandy soils and aquifer sediments. *Environ. Sci. Technol.* **2000**, *34*, 62−70.

(11) Xu, S.; Gao, B.; Saiers, J. E. Straining of colloidal particles in saturated porous media. *Water Resour. Res.* **2006**, *42*, W12S16 DOI: 10.1029/2006WR004948.

(12) Bradford, S. A.; Bettahar, M. Concentration dependent transport of colloids in saturated porous media. *J. Contam. Hydrol.* **2006**, *82*, 99−117.

(13) Ma, H.; Johnson, W. P. Colloid retention in porous media of various porosities: Predictions by the hemispheres-in-cell model. *Langmuir* **2010**, *26* (3), 1680−1687.

(14) Yoon, J. K.; Germaine, J. T.; Culligan, P. J. Visualization of particle behavior within a porous medium: Mechanisms for particle

filtration and retardation during downward transport. *Water Resour. Res.* **2006**, *42*, W06417 DOI: 10.1029/2004WR003660.
(15) Xu, S.; Liao, Q.; Saiers, J. E. Straining of nonspherical colloids in saturated porous media. *Environ. Sci. Technol.* **2008**, *42*, 771−778.
(16) Shen, C.; Lazouskaya, V.; Zhang, H.; Wang, F.; Li, B.; Jin, Y.; Huang, Y. Theoretical and experimental investigation of detachment of colloids from rough collector surfaces. *Colloids Surf., A* **2012**, *410*, 98−110.
(17) Ryan, J. N.; Gschwend, P. M. Effects of ionic strength and flow rate on colloid release: Relating kinetics to intersurface potential energy. *J. Colloid Intrerface Sci.* **1994**, *164*, 21−34.
(18) Li, X.; Johnson, W. P. Nonmonotonic variations in deposition rate coefficients of microspheres in porous media under unfavorable deposition conditions. *Environ. Sci. Technol.* **2005**, *39*, 1658−1665.
(19) Tong, M.; Ma, H.; Johnson, W. P. Funneling of flow into grain-to-grain contacts drives colloid-colloid aggregation in the presence of an energy barrier. *Environ. Sci. Technol.* **2008**, *42*, 2826−2832.
(20) Bradford, S. A.; Torkzaban, S.; Kim, H.; Simunek, J. Modeling colloid and microorganism transport and release with transients in solution ionic strength. *Water Resour. Res.* **2012**, *48*, W09509 DOI: 10.1029/2012WR012468.
(21) Grolimund, D.; Borkovec, M. Release of colloidal particles in natural porous media by monovalent and divalent cations. *J. Contam. Hydrol.* **2006**, *87*, 155−175.
(22) Tosco, T.; Tiraferri, A.; Sethi, R. Ionic strength dependent transport of microparticles in saturated porous media: Modeling mobilization and immobilization phenomena under transient chemical conditions. *Environ. Sci. Technol.* **2009**, *43*, 4425−4431.
(23) Kim, H. N.; Bradford, S. A.; Walker, S. L. *Escherichia coli* O157:H7 transport in saturated porous media: Role of solution chemistry and surface macromolecules. *Environ. Sci. Technol.* **2009**, *43*, 4340−4347.
(24) Wan, J.; Tokunaga, T.; Tsang, C. Bacterial sedimentation through a porous medium. *Water Resour. Res.* **1995**, *31* (7), 1627−1636.
(25) Chen, G.; Hong, Y.; Walker, S. L. Colloidal and bacterial deposition: Role of gravity. *Langmuir* **2010**, *26* (1), 314−319.
(26) James, S. C.; Chrysikopoulos, C. V. Dense colloid transport in a bifurcating fracture. *J. Colloid Interface Sci.* **2004**, *270*, 250−254, DOI: 10.1016/j.jcis.2003.09.033.
(27) James, S. C.; Chrysikopoulos, C. V. Monodisperse and polydisperse colloid transport in water-saturated fractures with various orientations: Gravity effects. *Adv. Water Resour.* **2011**, *34*, 1249−1255, DOI: 10.1016/j.advwatres.2011.06.001.
(28) Ma, H.; Pazmino, E. F.; Johnson, W. P. Gravitational settling effects on unit cell predictions of colloidal retention in porous media in the absence of energy barriers. *Environ. Sci. Technol.* **2011**, *45*, 8306−8312.
(29) Jin, Y.; Pratt, E.; Yates, M. Effect of mineral colloids on virus transport through saturated sand columns. *J. Environ. Qual.* **2000**, *29*, 532−540.
(30) Vasiliadou, I. A.; Chrysikopoulos, C. V. Cotransport of *Pseudomonas putida* and kaolinite particles through water saturated columns packed with glass beads. *Water Resour. Res.* **2011**, *47*, W02543 DOI: 10.1029/2010WR009560.
(31) Syngouna, V. I.; Chrysikopoulos, C. V. Cotransport of clay colloids and viruses in water saturated porous media. *Colloids Surf., A* **2013**, *416*, 56−65, DOI: 10.1016/j.colsurfa.2012.10.018.
(32) Katzourakis, V. E.; Chrysikopoulos, C. V. Mathematical modeling of colloid and virus cotransport in porous media: Application to experimental data. *Adv. Water Resour.* **2014**, *68*, 62−73, DOI: 10.1016/j.advwatres.2014.03.001.
(33) Silliman, S. E.; Dunlap, R.; Fletcher, M.; Schneegurt, M. A. Bacterial transport in heterogeneous porous media: Observations from laboratory experiments. *Water Resour. Res.* **2001**, *37* (11), 2699−2707.
(34) Chrysikopoulos, C. V.; Masciopinto, C.; La Mantia, R.; Manariotis, I. D. Removal of biocolloids suspended in reclaimed wastewater by injection in a fractured aquifer model. *Environ. Sci. Technol.* **2010**, *44* (3), 971−977, DOI: 10.1021/es902754n.
(35) Chrysikopoulos, C. V.; Syngouna, V. I.; Vasiliadou, I. A.; Katzourakis, V. E. Transport of *Pseudomonas putida* in a three-dimensional bench scale experimental aquifer. *Transp. Porous Media* **2012**, *94*, 617−642, DOI: 10.1007/s11242-012-0015-z.
(36) Thomas, J. M.; Chrysikopoulos, C. V. Experimental investigation of acoustically enhanced colloid transport in water-saturated packed columns. *J. Colloid Interface Sci.* **2007**, *308* (1), 200−2007, DOI: 10.1016/j.jcis.2006.12.062.
(37) Kretzschmar, R.; Barmettler, K.; Grolimund, D.; Yan, Y. D.; Borkovec, M.; Sticher, H. Experimental determination of colloid deposition rates and collision efficiencies in natural porous media. *Water Resour. Res.* **1997**, *33* (5), 1129−1137.
(38) Jin, Y.; Chu, Y.; Li, Y. Virus removal and transport in saturated and unsaturated sand columns. *J. Contam. Hydrol.* **2000**, *43* (2), 111−128.
(39) Chu, Y.; Jin, Y.; Baumann, T.; Yates, M. V. Effect of soil properties on saturated and unsaturated virus transport through columns. *J. Environ. Qual.* **2003**, *32*, 2017−2025.
(40) Bradford, S. A.; Simunek, J.; Walker, S. L. Transport and straining of *E. coli* O157:H7 in saturated porous media. *Water Resour. Res.* **2006**, *42*, W12S12 DOI: 10.1029/2005WR004805.
(41) Anders, R.; Chrysikopoulos, C. V. Transport of viruses through saturated and unsaturated columns packed with sand. *Transp. Porous Media* **2009**, *76*, 121−138, DOI: 10.1007/s11242-008-9239-3.
(42) Sinton, L. W.; Mackenzie, M. L.; Karki, N.; Dann, R. L.; Pang, L.; Close, M. E. Transport of *Escherichia coli* and F-RNA bacteriophages in a 5-m column of saturated, heterogeneous gravel. *Water, Air, Soil Pollut.* **2012**, *223*, 2347−2360.
(43) Bolster, C. H.; Mills, A. L.; Hornberger, G. M.; Herman, J. S. Spatial distribution of diposited bacteria following miscible displacement experiments in intact cores. *Water Resour. Res.* **1999**, *35* (6), 1797−1807.
(44) Compere, F.; Porel, G.; Delay, F. Transport and retention of clay particles in saturated porous media: Influence of ionic strength and pore velocity. *J. Contam. Hydrol.* **2001**, *49*, 1−21.
(45) Schijven, J. F.; Hassanizadeh, S. M.; de Bruin, R. H. A. M. Two-site kinetic modeling of bacteriophages transport through columns of saturated dune sand. *J. Contam. Hydrol.* **2002**, *57*, 259−279.
(46) Hahn, M. W.; Abadzic, D.; O'Melia, C. R. Aquasols: On the role of secondary minima. *Environ. Sci. Technol.* **2004**, *38*, 5915−5924.
(47) Mitropoulou, P. N.; Syngouna, V. I.; Chrysikopoulos, C. V. Transport of colloids in unsaturated packed columns: Role of ionic strength and sand grain size. *Chem. Eng. J.* **2013**, *232*, 237−248, DOI: 10.1016/j.cej.2013.07.093.
(48) Happel, J. Viscous flow in multiparticle systems: Slow motion of fluids relative to beds of spherical particles. *AIChE J.* **1958**, *4*, 197−201.
(49) Ma, H.; Pedel, J.; Fife, P.; Johnson, W. P. Hemispheres-in-cell geometry to predict colloid deposition in porous media. *Environ. Sci. Technol.* **2009**, *43*, 8573−8579.
(50) Sim, Y.; Chrysikopoulos, C. V. Analytical models for one-dimensional virus transport in saturated porous media. *Water. Resour. Res.* **1995**, *31*, 1429−1437, DOI: 10.1029/95WR00199; Correction. *Water Resour. Res.* **1996**, *32*, 1473 DOI: 10.1029/96WR00675.
(51) Russel, W. B.; Saville, D. A.; Schowlter, W. R. *Colloidal Dispersions*; Cambridge University Press: Cambridge, UK, 525 pp 1989.
(52) Sim, Y.; Chrysikopoulos, C. V. Three-dimensional analytical models for virus transport in saturated porous media. *Transp. Porous Media* **1998**, *30*, 87−112, DOI: 10.1023/A:1006596412177.
(53) Sim, Y.; Chrysikopoulos, C. V. Analytical solutions for solute transport in saturated porous media with semi-infinite or finite thickness. *Adv. Water Resour.* **1999**, *22*, 507−519, DOI: 10.1016/S0309-1708(98)00027-X.
(54) Chrysikopoulos, C. V.; Roberts, P. V.; Kitanidis, P. K. One-dimensional solute transport in porous media with partial well-to-well recirculation: Application to field experiments. *Water Resour. Res.* **1990**, *26*, 1189−1195, DOI: 10.1029/89WR03629.

(55) Pruett, R. J.; Webb, H. L. Sampling and analysis of KGa-1b well-crystallized kaolin source clay. *Clays Clay Miner.* **1993**, *41* (4), 514−519.
(56) Van Olphen, H.; Fripiat, J. J. *Data Handbook for Clay Minerals and Other Non-Metallic Minerals*; Pergamon Press: Oxford, England, 1979.
(57) Sanders, R. L.; Washton, N. M.; Mueller, K. T. Measurement of the reactive surface area of clay minerals using solid-state NMR studies of a probe molecule. *J. Phys. Chem. C* **2010**, *114* (12), 5491−5498.
(58) Rong, X.; Huanga, Q.; He, X.; Chen, H.; Cai, P.; Liang, W. Interaction of *Pseudomonas putida* with kaolinite and montmorillonite: A combination study by equilibrium adsorption, ITC, SEM and FTIR. *Colloids Surf., B* **2008**, *64*, 49−55.
(59) Chrysikopoulos, C. V.; Syngouna, V. I. Attachment of bacteriophages MS2 and ΦX174 onto kaolinite and montmorillonite: Extended-DLVO interactions. *Colloids Surf., B* **2012**, *92*, 74−83, DOI: 10.1016/j.colsurfb.2011.11.028.
(60) Wu, W. Baseline studies of the clay minerals society source clays: Colloid and surface phenomena. *Clays Clay Miner.* **2001**, *49*, 446−452.
(61) Shahidzadeh-Bonn, N.; Tournié, A.; Bichon, S.; Vié, P.; Rodts, S.; Faure, P.; Bertrand, F.; Azouni, A. Effect of wetting on the dynamics of drainage in porous media. *Transp. Porous Media* **2004**, *56*, 209−224.
(62) Basha, H. A.; Culligun, P. J. Modeling particle transport in downward and upward flows. *Water Resour. Res.* **2010**, *46*, W07518 DOI: 10.1029/2009WR008133.
(63) van Oss, C. J.; Good, R. J.; Chaudhury, M. K. The role of van der Waals forces and hydrogen bonds in "hydrophobic interactions" between biopolymers and low energy surfaces. *J. Colloid Interface Sci.* **1986**, *111*, 378−390.
(64) van Oss, C. J.; Giese, R. F. Role of the properties and structure of liquid water in colloidal and interracial systems. *J. Dispersion Sci. Technol.* **2004**, *25* (5), 631−655.
(65) Johnson, W. P.; Pazmino, E.; Ma, H. Direct observations of colloid retention in granular media in the presence of energy barriers, and implications for inferred mechanisms from indirect observations. *Water Res.* **2010**, *44*, 1158−1169.
(66) Seymour, M. B.; Chen, G.; Su, C.; Li, Y. Transport and retention of colloids in porous media: Does shape really matter? *Environ. Sci. Technol.* **2013**, *47*, 8391−8398.
(67) Shellenberger, K.; Logan, B. E. Effect of molecular scale roughness of glass beads on colloidl and bacterial deposition. *Environ. Sci. Technol.* **2002**, *36*, 184−189.
(68) Saiers, J. E.; Ryan, J. N. Colloid deposition on non-ideal porous media: The influences of collector shape and roughness on the single-collector efficiency. *Geophys. Res. Lett.* **2005**, *32*, L21406 DOI: 10.1029/2005GL024343.
(69) Auset, M.; Keller, A. A. Pore-scale visualization of colloid straining and filtration in saturated porous media using micromodels. *Water Resour. Res.* **2006**, *42*, W12S02 DOI: 10.1029/2005WR004639.
(70) Shen, C.; Wang, F.; Li, B.; Jin, Y.; Wang, L.-P.; Huang, Y. Application of DLVO energy map to evaluate interactions between spherical colloids and rough surfaces. *Langmuir* **2012**, *28*, 14681−14692.
(71) Chrysikopoulos, C. V.; Abdel-Salam, A. Modeling colloid transport and deposition in saturated fractures. *Colloids Surf., A* **1997**, *121*, 189−202, DOI: 10.1016/S0927-7757(96)03979-9.